

Band Gap Energy of Periodic Anatase TiO₂ System Evaluated with the B2PLYP Double Hybrid Functional

Siti Hajar Alias^a, Fazira Ilyana Abdul Razak^b, Sheela Chandren^b, Wai Loon Leaw^b, Riadh Sahnoun^c, Hadi Nur^{d*}

^aAdvanced Material for Environmental Remediation (AMER) Research Group, Faculty of Applied Sciences, Universiti Teknologi MARA Cawangan Negeri Sembilan Kampus Kuala Pilah, 72000 Kuala Pilah, Negeri Sembilan, Malaysia;

^bDepartment of Chemistry, Faculty of Science, Universiti Teknologi Malaysia, 81310 UTM Johor Bahru, Johor, Malaysia; ^cDepartment of Chemistry, Baze University, Abuja, Nigeria; ^dCenter of Advanced Materials for Renewable Energy (CAMRY), Universitas Negeri Malang, Malang 65145, Indonesia

Abstract The electronic properties of anatase titanium dioxide (TiO₂) materials are of paramount importance for photocatalytic application. Ab initio calculation is performed on anatase TiO₂ with various cluster sizes and shape, using Gaussian 09 program employing the standard 6-311G(d) and 3-21G basis set. Hartree-Fock (HF) theory, exchange-functional of density functional theory including hybrid (B3LYP, B3PW91, PBE1PBE and PBEh1PBE) and double-hybrid (B2PLYP), together with 2nd order Møller-Plesset perturbation theory are used to predict the band gap energy of anatase TiO₂. With the inclusion of long-range HF exchange, double hybrid B2PLYP functional is able to predict band gap energy value (3.06 eV) which as compared to the experimental value (3.20 eV). Besides, this double hybrid exchange-correlation functional shows good compromise by obtaining an accurate description for cohesive energy of anatase TiO₂. Thus, double-hybrid B2PLYP functional is suggested to be a practical choice for predicting the electronic properties for anatase TiO₂.

Keywords: B2PLYP, band gap energy TiO₂, double hybrid functional.

Introduction

TiO₂ has attracted particular attention of scientists in 1971 when Fujishima and Honda demonstrated the potential of TiO₂ in photocatalytic water splitting using TiO₂ semiconductor electrode [1,2]. Titanium dioxide is also considered to be an excellent and promising material in paints pigments, degradation of water pollutants, electrochromic displays, electrochemical electrodes, capacitors, lithium-ion batteries, air purification, dye-sensitized solar cell (DSSC) electrodes, sensors and catalysts' support due to its high specific surface area, low material cost, excellent stability, outstanding photocatalytic activity, stability towards photo-corrosion, and being environmental friendly and nontoxic [3–6].

In brief, TiO₂ is a semiconducting metal oxide that can be found in three different polymorphs in nature: anatase, rutile, and brookite. It is reported that TiO₂ has a relatively large band gap of 3.20 eV for the anatase phase and 3.03 eV for rutile phase [7,8]. Anatase phase has received more attention in numerous experimental and theoretical studies over the years due to its superior photocatalytic properties and high technological application. Abundant literature is, therefore, focused on the synthesis of the anatase TiO₂ using various methods or techniques to modify the band gap energy of anatase TiO₂ varies from 2.78 to 3.24 eV depending on the preparation method, as well as the effect of dopant [9], oxygen vacancy [10] and etc. (full details provided in supplementary information).

*For correspondence:
hadinur.fmipa@um.ac.id

Received: 13 Oct. 2023

Accepted: 1 Jan. 2024

©Copyright Alias. This article is distributed under the terms of the [Creative Commons Attribution License](#), which permits unrestricted use and redistribution provided that the original author and source are credited.

Comply with experimental research work, computation is also intensively performed to define the electronic properties of TiO₂. For instance, Kohn-Sham density functional theory (DFT) has been widely used in the solid-state community for electronic structure calculations. It is reported being able to describe the structural properties of TiO₂. However, Kohn-Sham DFT that applies an exchange and correlation potential approximation for the description of the band gap energy gives unsatisfactory result due to the self-interaction error [11,12] and delocalization error.

On the other hands, some studies [13–18] which are based on the standard exchange-correlation functional LDA and GGA approach, underestimate the band gap energy for about 2.0 to 2.6 eV compared to the experimental value of 3.2 eV as shown in Table 1. This general trend is the major band gap problem in DFT based calculations. Compared to standard LDA or GGA functionals, hybrid functionals that include some exact Hartree-Fock exchange (B3LYP, B3PW91, PBE0, etc.) provide improved band gap values of TiO₂. This is due to that fact that hybrid functionals partly correct the self-interaction error inherent in DFT. Self-interaction error is the interactions of electrons that basically should not exist as based on Pauli exclusion principle [19,20].

In addition, delocalization error is also another dominant and fundamental error that affects the density functional approximation. Delocalization error which was defined by Mori-Sánchez et. al [23] as the ground state energy system as a function of electron number $E(N)$, should be a straight-line interpolating between integers. Deviation from this straight-line behavior represents an error that is a convex curve for the total energy $E(N)$. This convex curve is obtained from density functional approximations. Conversely, a concave curve, as obtained from Hartree-Fock (HF) represents a localization error. In this case, inclusion of long-range HF exchange in hybrid and double-hybrid functionals often makes $E(N)$ curves straighter, and hence the range-separated density functional approximations have a less severe delocalization error. Therefore, the accuracy of the band gap energy increases with the increase of the percentage of HF exchange [11,21,22].

Previous study found that hybrid functional B3PW91 improved the band gap energy for the binary and ternary semiconductor compounds compared to the other hybrid functionals including B3LYP and PBE0. They found that B3LYP functionals underestimate the band gap energy due to the underestimated correlation energy of the uniform electron gas by 30% compared to the B3PW91. In contrary, Labat et. al and Di Valenti et. al [22,23] whom used different computational parameters, obtained an overestimated band gap energy of 3.98 and 3.90 eV, respectively. A modified hybrid functional PBEx has been proposed by Kyoung et. al. [12], which contain a 12.5% of Fock exchange produces the experimental band gap energy about 3.19 eV.

Table 1. Summary of optimized lattice parameters, calculated band gaps and percent band gap error reported in previous works according to DFT approaches

No of atom	Computational Package	Exchange-Correlation Functional	Basis Set	Optimized Lattice Parameters (Å)		Band Gap (eV)	Band Gap Error (%)	Reference
				a, b	c			
GGA and LDA Functional								
24	CASTEP	PBE-GGA	Plane-wave	3.792	9.742	2.23	31.25	[15]
32	CASTEP	PBE-GGA	Plane-wave	3.806	9.659	2.12	33.75	[16]
48	VASP	PW91-GGA	Pseudopotential	3.771	9.411	2.00	37.50	[17]
48	CASTEP	PW91-GGA	Pseudopotential	3.800	9.790	2.19	31.56	[18]
48	CASTEP	PBE-GGA	Plane-wave	3.748	9.712	2.25	29.69	[19]
48	CASTEP	LDA	Plane-wave	3.785	9.481	2.54	20.63	[20]
Hybrid Functional								
32	CRYSTAL and VASP	B3LYP	Gaussian and projected plane wave	3.783	9.805	3.98	24.38	[25]
96	CRYSTAL	B3LYP	Gaussian Type Orbitals	3.776	9.866	3.90	21.88	[24]
Modified Hybrid Functional								
95	FHI-aims	PBEx	Light grid/Tier-1	3.799	9.702	3.19	0.30	[14]

The double-hybrid B2PLYP method is in fifth rungs of Jacob’s ladder of density functional theory approximation that uses unoccupied orbitals and eigenvalues in functionals. It appears as a promising alternative as it has already been shown to provide accurate results even for excited states [24]. This functional is a reparametrized B3LYP hybrid mixed with MP2 correlation with the eigenvalues correspond to the excited states. In the current work, we report the performance of HF and five popular exchange-

correlation functionals of DFT including hybrid (B3LYP, B3PW91, PBE1PBE or known as PBE0 and PBEh1PBE), double-hybrid functional (B2PLYP) and MP2 that is available in Gaussian 09 package in predicting band gap energy. The cohesive energy for various anatase clusters is also examined due to its importance in determining the phase stability for the anatase TiO₂ cluster. The results presented here include the density of states and Mulliken charge transfer. Here, we demonstrate that the double hybrid B2PLYP with 6-311G(d) or 3-21G basis set using Gaussian 09 package are satisfactory to study the trend of the electronic structure of anatase TiO₂ due to the good estimation of the band gap energy compared to the hybrid functional of B3LYP, B3PW91, PBE1PBE and PBEh1PBE.

Computational Details

The computational calculation was carried out using Gaussian 09 series of programs [25]. All the calculations employed the Pople-type split valence basis set 6-311G(d) and 3-21G as implemented in these programs. The anatase TiO₂ geometries that have been used are those of the experimentally determined structural parameters from literature with unit cell parameters of $a = b = 3.785 \text{ \AA}$, $c = 9.514 \text{ \AA}$, $u = 0.2066 \text{ \AA}$. The anatase TiO₂ structure belongs to the tetragonal space group I41/amd and each atom in anatase TiO₂ is octahedrally coordinated to six oxygen atoms [26]. We selected a series of finite anatase nanoparticles clusters Ti₁₃O₁₈, Ti₂₁O₃₀, Ti₂₉O₄₂, Ti₃₄O₅₀, Ti₅₉O₁₀₀, Ti₆₅O₉₈ and Ti₁₆₃O₂₉₄ to study the structural and electronic properties of anatase TiO₂ cluster (Table 2). Molden software was used for visualization of anatase TiO₂ cluster [27].

Table 2. Description of TiO₂ cluster

TiO ₂ cluster	Total number of atoms	Unit cell (xyxz)	Symmetry
Ti ₁₃ O ₁₈	31	1x1x1	<i>D</i> _{2d}
Ti ₂₁ O ₃₀	51	2x1x1	<i>C</i> _{2v}
Ti ₂₉ O ₄₂	71	3x1x1	<i>D</i> _{2d}
Ti ₃₄ O ₅₀	84	2x2x1	<i>D</i> _{2d}
Ti ₅₉ O ₁₀₀	159	2x2x2	<i>D</i> _{2d}
Ti ₆₅ O ₉₈	163	3x3x1	<i>D</i> _{2d}
Ti ₁₆₃ O ₂₉₄	457	3x3x3	<i>D</i> _{2d}

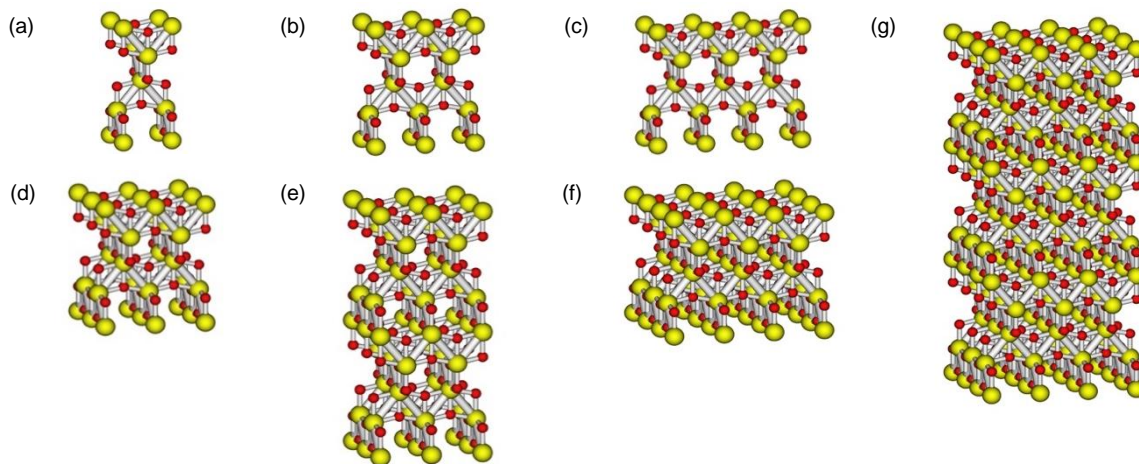


Figure 1. Cluster models of anatase TiO₂ (a) Ti₁₃O₁₈, (b) Ti₂₁O₃₀, (c) Ti₂₉O₄₂, (d) Ti₃₄O₅₀, (e) Ti₅₉O₁₀₀, (f) Ti₆₅O₉₈, and (g) Ti₁₆₃O₂₉₄ (yellow spheres and red spheres are Ti and O atoms, respectively)

A variety of levels of theory have been used in order to assess the reliability of the selected theories. HF [28], DFT method of Hybrid Functional-B3LYP [29–31], B3PW91 [29,32–34], PBE1PBE [35–37], PBEh1PBE [35,36,38], double-hybrid density functional of B2PLYP [39] and 2nd order Møller-Plesset Perturbation Theory, MP2 [40–43] were among the selected theories. The band gap is calculated from the difference in the orbital energies of the LUMO and the HOMO. HOMO is occupied orbital while LUMO

is unoccupied orbital or virtual orbital obtained from a single point calculation. To evaluate the accuracy of calculated HOMO-LUMO energy, error percentage was calculated using equation 1.

$$E_g \text{ error (\%)} = \frac{|E_g(\text{exp}) - E_g(\text{theory})|}{E_g(\text{exp})} \times 100 \quad (1)$$

where $E_{g(\text{exp})}$ is the experimental band gap energy that is 3.20 eV and $E_{g(\text{theory})}$ is the calculated band gap energy from various ab-initio methods.

For studying the effect of lattice parameter on the band gap energy of anatase TiO₂ cluster, we calculate the band gap energy difference between band gap energy for pure anatase cluster without structural distortion and band gap energy for anatase with structural distortion (eqn. 2).

$$\Delta E_g = E_{g(\text{pure})} - E_{g(\text{theory})} \quad (2)$$

where $E_{g(\text{pure})}$ is the calculated band gap energy for pure anatase without any structural distortion (0 Å) and $E_{g(\text{theory})}$ is the calculated band gap energy with structural distortion.

The cohesive energy for all anatase TiO₂ cluster at different types of ab initio methods and basis sets was evaluated. The cohesive energy or binding energy is defined as the energy required to break all the bonds into separate parts [44]. The anatase cluster structure which shows the lowest cohesive energy is proposed to be the most stable phase. The absolute value of total cohesive energy, E_c (eV), absolute value of cohesive energy per atom, $E_{c / \text{atom}}$ (eV/atom), absolute value of cohesive energy per TiO₂ formula unit, E_{c / TiO_2} (eV/TiO₂) of the anatase clusters was calculated using the eqn. 3, 4 and 5, respectively. The symbol m represents the number of Ti atoms while n represents the number of O atoms in the cluster.

$$E_c \text{ (eV)} = E_{(\text{Ti}_m\text{O}_n)} - (mE_{\text{Ti}} + nE_{\text{O}}) \quad (3)$$

$$E_{c / \text{atom}} \text{ (eV/atom)} = \frac{E_c \text{ (eV)}}{m+n} \quad (4)$$

$$E_{c / \text{TiO}_2} \text{ (eV/TiO}_2) = E_c \text{ (eV/atom)} \times 3 \text{ (atom/TiO}_2 \text{ formula unit)} \quad (5)$$

Results and discussion

Cluster Modeling of Anatase

Figure 1 shows the different cluster models that were used in this work. One primitive unit supercell (Ti₁₃O₁₈) consisted of 13 Ti atoms and 18 O atoms with the apical Ti-O bond length being slightly longer (1.96559 Å) than the equatorial Ti-O bond length (1.93702 Å). All the cluster models have symmetry D_{2d} except Ti₂₁O₃₀ symmetry C_{2v} , as shown in Table 2.

Performance of the Theoretical Methods in the Calculation of Band Gap Energy and Cohesive Energy of Anatase Cluster

Table 3 shows the total energy, absolute value of cohesive energy, the absolute value of cohesive energy per atom, the absolute value of cohesive energy per TiO₂ formula unit, band gap energy and percent band gap error for Ti₁₃O₁₈ to Ti₁₆₃O₂₉₄ clusters varied with size calculated at HF, MP2 and different DFT methods employing 6-311G(d) basis set. Overall, double-hybrid B2PLYP functional produced band gap energies with lowest error percentages among the cluster models from Ti₁₃O₁₈ to Ti₃₄O₅₀. For larger cluster models of Ti₅₉O₁₀₀ and Ti₆₅O₉₈, none of the methods produce acceptable band gap energy. Remarkably, double-hybrid B2PLYP functional produced band gap energy of 3.06 eV with the lowest error percentage of 4.38 % by using Ti₂₁O₃₀ anatase as a cluster model. In contrary, B3LYP hybrid functional which is conventionally studied with different computational parameters [22,23] produced underestimated value with a gap difference of 0.74 eV and error percentage as large as of ~77%.

Table 3. Total energy, E (a.u.), absolute value of total cohesive energy, E_c (eV), absolute value of cohesive energy per atom, $E_c / atom$ (eV/atom), absolute value of cohesive energy per TiO₂ formula unit, E_c / TiO_2 (eV/TiO₂), theoretical band gap energy, E_g (eV) and band gap error (%) for anatase, TiO₂ clusters calculated at HF and different DFT methods/6-311G(d)

Structure	Method	E	E_c	$E_c / atom$	E_c / TiO_2	E_g	E_g Error
Ti ₁₃ O ₁₈	B3LYP	-12398.199562	215.56	6.95	20.85	1.38	56.88
	B3PW91	-12396.815742	220.86	7.12	21.36	1.43	55.31
	PBE1PBE	-12393.831826	220.43	7.11	21.33	1.74	45.63
	PBEh1PBE	-12394.283436	220.35	7.11	21.33	1.75	45.31
	B2PLYP	-12393.656174	216.46	6.98	20.94	3.57	11.56
	HF	-12377.267248	148.01	4.77	14.31	5.66	76.88
	MP2	-12382.479843	216.08	6.97	20.91	5.66	76.88
Ti ₂₁ O ₃₀	B3LYP	-20097.814434	368.31	7.22	21.66	0.74	76.88
	B3PW91	-20095.561790	377.31	7.40	22.2	0.76	76.25
	PBE1PBE	-20090.718430	377.23	7.40	22.2	1.14	64.38
	PBEh1PBE	-20091.456690	377.12	7.39	22.17	1.13	64.69
	B2PLYP	-20090.444877	370.30	7.26	21.78	3.06	4.38
	HF	-20063.726539	259.39	5.09	15.27	5.86	83.13
	MP2	-20072.347691	371.53	7.28	21.84	5.86	83.13
Ti ₂₉ O ₄₂	B3LYP	-27797.441419	521.38	7.34	22.02	0.79	75.31
	B3PW91	-27794.318604	534.06	7.52	22.56	0.81	74.69
	PBE1PBE	-27787.598053	533.84	7.52	22.56	0.86	73.13
	PBEh1PBE	-27788.624046	533.73	7.52	22.56	0.86	73.13
	B2PLYP	-27787.224569	523.89	7.38	22.14	2.81	12.19
	HF	-27749.653025	356.27	5.02	15.06	1.55	51.56
	MP2	-27762.5841858	537.00	7.56	22.68	1.55	51.56
Ti ₃₄ O ₅₀	B3LYP	-32647.626570	628.66	7.48	22.44	0.81	74.69
	B3PW91	-32643.957183	644.06	7.67	23.01	0.82	74.38
	PBE1PBE	-32636.057305	644.26	7.67	23.01	1.09	65.94
	PBEh1PBE	-32637.268020	644.16	7.67	23.01	1.08	66.25
	B2PLYP	-32635.648769	632.74	7.53	22.59	2.71	15.31
	HF	-32592.068637	454.17	5.41	16.23	5.29	65.31
	MP2	-32606.2854771	637.67	7.59	22.77	5.29	65.31
Ti ₅₉ O ₁₀₀	B3LYP	-	-	-	-	-	-
	B3PW91	-	-	-	-	-	-
	PBE1PBE	-57630.542898	1283.88	8.07	24.21	0.31	90.31
	PBEh1PBE	-57632.753326	1283.58	8.07	24.21	0.31	90.31
	B2PLYP	-	-	-	-	-	-
	HF	-57549.990500	918.20	5.77	17.31	5.37	67.81
	MP2	-	-	-	-	-	-
Ti ₆₅ O ₉₈	B3LYP	-62597.439340	1256.74	7.71	23.13	0.40	87.50
	B3PW91	-	-	-	-	-	-
	PBE1PBE	-62575.205361	1289.04	7.91	23.73	0.21	93.44
	PBEh1PBE	-62577.543297	1288.92	7.91	23.73	0.53	83.44
	B2PLYP	-	-	-	-	-	-
	HF	-62490.562001	925.14	5.68	17.04	4.84	51.25
	MP2	-	-	-	-	-	-
Ti ₁₆₃ O ₂₉₄	B3LYP	-	-	-	-	-	-
	B3PW91	-	-	-	-	-	-
	PBE1PBE	-160555.419488	3846.17	8.42	25.26	0.24	92.50
	PBEh1PBE	-	-	-	-	-	-
	B2PLYP	-	-	-	-	-	-
HF	-160327.887867	2805.95	6.14	18.42	4.92	53.75	
MP2	-	-	-	-	-	-	

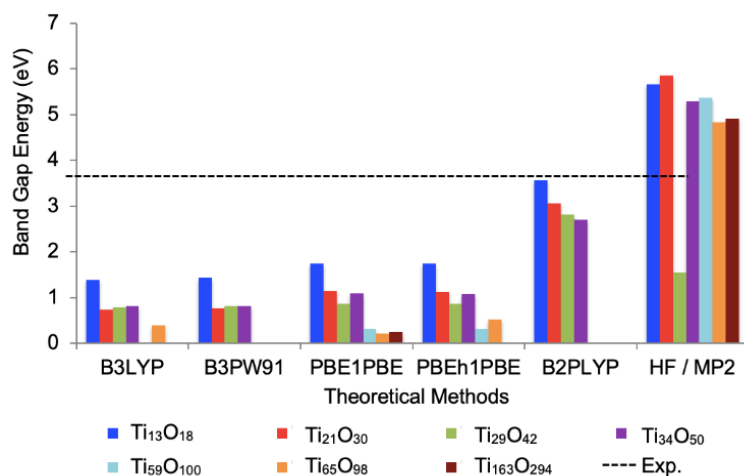


Figure 2. Band gap energy of anatase TiO₂ cluster versus HF, MP2 and various DFT theoretical methods with 6-311G(d) basis set

All the calculated band gap energies from different theoretical methods and cluster models were plotted as bar chart as shown in Figure 2 in order to show the trend of band gap energy as affected by the degree of HF exchange in each theoretical method. It is clear that the HF method overestimated the band gap energy compared to the experimental value because of the correlation contribution was neglected. On the other hands, the hybrid functionals B3LYP and B3PW91 with a minor inclusion of 20% of HF exchange underestimate the band gap energy of TiO₂. While PBE1PBE hybrid functional with an addition of 25% of HF exchange to the standard PBE form of the GGA functionals improve the band gap energy of anatase TiO₂. With a minor inclusion of HF exchange, band gap energy of anatase TiO₂ is underestimated compared to the experimental value of 3.20 eV, due to the well-known limitation of the generalized gradient approximation (GGA) [45] and due to the well-known shortcoming of the exchange-correlation functional in describing excited states [13,46]. However, an important trend was found that the calculated band gaps could be improved with the adjustment of the percentage of HF exchange. This is because the HF exchange could lead to some degree of cancellation between the delocalization and localization errors and it is certainly an important factor in obtaining accurate band gaps [11,21,22]. Hence, the outcome from double-hybrid B2PLYP density functionals is in-line with the discussion. Double-hybrid B2PLYP density functional which is based on the mixing of standard generalized gradient approximations (GGAs) for exchange and correlation with a large amount of HF exchange (~50%) and a perturbative second-order correlation part (PT2) that is obtained from the Kohn-Sham (GGA) orbitals and eigenvalues, brings the computational band gap energy value close to the experimental value. With an inclusion of higher degree of HF exchange, the related errors including the self-interaction error and delocalization error are significantly reduced.

The band gap energy generated by B2PLYP is cluster size dependent. The band gap energy decreases from 3.57 eV for Ti₁₃O₁₈, 3.06 eV for Ti₂₁O₃₀, 2.81 eV for Ti₂₉O₄₂, to 2.71 eV for Ti₃₄O₅₀. B3LYP, PBE1PBE and PBEh1PBE functional shows the same trend except B3PW91 functional which are not known due to the difficulty to converge for Ti₅₉O₁₀₀ to Ti₁₆₃O₂₉₄ anatase cluster. Mori-Sánchez and co-workers [21] reported that the delocalization error is size-dependent for all exchange-correlation functional. They stated that in finite systems calculations, the delocalization error increase with system size until it stabilizes at a certain system size. Hence, the band gap energy becomes linear at infinite size due to the maximum delocalization and localization error, and it can be determined using periodic boundary calculations [21]. The periodic boundary calculations have been tried; however, this calculation demands a large amount of memory and it becomes a limitation in our study. From these finding, it shows that none of the existing density functional approximations is capable of predicting band gaps with consistent accuracy for the system of all sizes [47]. However, calculation using B2PLYP based in small cluster is suggested as a practical approach.

The band gap energy calculated using B2PLYP was validated by calculating the cohesive energy for anatase TiO₂ clusters. In general, the cohesive energy increases as the size of the cluster increases. This is because as the cluster becomes larger, the cohesive energy increases due to the increase on the coordination number of the atoms in the cluster. As recorded in Table 3, the cohesive energy per TiO₂ formula unit is located in between 20.85 to 23.01 eV for all DFT functionals based on small to medium cluster (Ti₁₃O₁₈-Ti₃₄O₅₀), which is in good agreement with literature values reported for around 21.54 to 22.54 eV [48–50]. In particular, the cohesive energy per TiO₂ formula unit calculated using

B2PLYP is 20.94 - 22.59 eV. The HF method is not excepted due to its underestimated value. Hence, the functionality of B2PLPY is again proven.

The basis set was then reduced to B2PLYP/3-21G for further study of anatase $\text{Ti}_{59}\text{O}_{100}$ cluster due to memory limitations at B2PLYP/6-311G(d) levels. The full details on the comparison of total energy, the absolute value of total cohesive energy, cohesive energy per atom, the band gap energy and percentage band gap energy error between B2PLYP/6-311G(d) and B2PLYP/3-21G level of DFT for all anatase TiO_2 clusters are provided in Table 4. Table 4 shows that the band gap energy for all anatase TiO_2 cluster was narrowed when the basis set changes from 6-311G(d) to the 3-21G basis set. Moreover, for cohesive energy, the cohesive energy per atom increases when the basis set is reduced to 3-21G. It was reasonable to say that a higher number of basis functions and the inclusion of polarization functions significantly enhance the quality and possibly the accuracy of the results despite the fact that 6-311G(d) required more CPU time and higher memory to complete the calculation compared to the 3-21G basis set. In short, calculation using B2PLYP/6-311G(d) is still preferable.

Impact of Structure Distortion on the Performance of Theoretical Methods in the Calculation of Band Gap Energy and Cohesive Energy of Anatase Cluster of TiO_2

Experimental work shows that during the synthesis of anatase TiO_2 , the lattice parameter differs slightly, maybe due to the addition of dopants and etc (details provided in supplementary information). Therefore, in this section, we assessed the calculation of the band gap energy using B2PLYP functional at different lattice parameters resembling geometry optimization of the TiO_2 crystal structure. Technically, the geometry optimization usually attempts for the smallest structure to predict the equilibrium structures of molecular systems by locating the minima of the potential energy surface. In this work, the optimization is therefore based on the $\text{Ti}_{13}\text{O}_{18}$ cluster. By resembling the optimization, the Ti-O bond length has been increase at x, y and z-axis range from -0.10 Å to 0.10 Å, resulting in the structural distortion of the anatase TiO_2 cluster, that is breathing and shrinking mode of anatase cluster.

Figure 3 shows the variation of the absolute energy versus distortion $\text{Ti}_{13}\text{O}_{18}$ cluster at B2PLYP/6-311G(d). As observed from the variation of the absolute energy in Figure 3, distortion at -0.06 Å has the lowest energy and highest cohesive energy per atom which indicates that distortion anatase at -0.06 Å is more stable than other structural distortion value. Table 5 shows the lattice parameters, total energy, the absolute value of total cohesive energy, the absolute value of cohesive energy per atom and band gap energy at a different value of structural distortion, r , for anatase $\text{Ti}_{13}\text{O}_{18}$ cluster calculated at B2PLYP/6-311G(d). The change of band gap energy is small that is only 0.15 eV for $\text{Ti}_{13}\text{O}_{18}$. Hence, it is assumed that B2PLYP/6-311G(d) is suitable for practical use.

Table 4. Total energy, E (a.u.), absolute value of total cohesive energy, E_c (eV), absolute value of cohesive energy per atom, $E_c / atom$ (eV/atom), theoretical band gap energy, E_g (eV) and band gap energy error (%) calculated at B2PLYP/6-311G(d) and B2PLYP/3-21G level of DFT for anatase TiO_2 cluster models

Anatase TiO_2 Cluster	Basis Set	E	E_c	$E_c / atom$	E_g
$\text{Ti}_{13}\text{O}_{18}$	6-311G(d)	-12393.656174	216.46	6.98	3.57
	3-21G	-12333.158664	234.15	7.55	3.29
$\text{Ti}_{21}\text{O}_{30}$	6-311G(d)	-20090.444877	370.30	7.26	3.06
	3-21G	-19992.419646	401.85	7.88	2.82
$\text{Ti}_{29}\text{O}_{42}$	6-311G(d)	-27787.224569	523.89	7.38	2.81
	3-21G	-27651.677361	569.45	8.02	2.51
$\text{Ti}_{34}\text{O}_{50}$	6-311G(d)	-32635.648769	632.74	7.53	2.71
	3-21G	-32476.522021	689.58	9.71	2.51
$\text{Ti}_{59}\text{O}_{100}$	6-311G(d)	-	-	-	-
	3-21G	-57348.620729	1371.90	8.63	2.53
$\text{Ti}_{65}\text{O}_{98}$	6-311G(d)	-	-	-	-
	3-21G	-62269.598911	1385.91	8.50	2.16

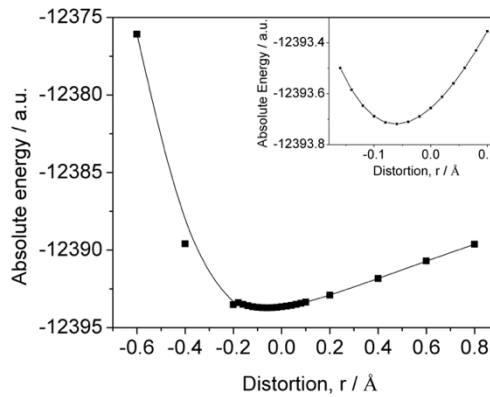


Figure 3. Variation of the absolute energy versus distortion of $Ti_{13}O_{18}$ cluster at B2PLYP/6-311G(d)

Table 5. Total energy, E (a.u.), absolute value of total cohesive energy, E_c (eV), absolute value of cohesive energy per atom, $E_c / atom$ (eV/atom) and theoretical band gap energy, E_g (eV) at different value of structural distortion, r (Å), for anatase $Ti_{13}O_{18}$ cluster at B2PLYP/6-311G(d) level

r	lattice parameters		$Ti_{13}O_{18}$				
	a, b	c	E	E_c	$E_c / atom$	E_g	ΔE_g
-0.10	3.5472	9.3769	-12393.6887571	217.34	7.01	3.27	0.30
-0.08	3.5955	9.4038	-12393.7125110	217.99	7.03	3.35	0.22
-0.06	3.6435	9.4309	-12393.7187668	218.16	7.04	3.42	0.15
-0.04	3.6911	9.4584	-12393.7106545	217.94	7.03	3.48	0.09
-0.02	3.7382	9.4861	-12393.6893081	217.36	7.01	3.53	0.04
0.00	3.7850	9.5120	-12393.6561738	216.46	6.98	3.57	0.00
0.02	3.8314	9.5422	-12393.6125404	215.27	6.94	3.56	0.01
0.04	3.8775	9.5706	-12393.5595732	213.83	6.90	3.52	0.05
0.06	3.9233	9.5993	-12393.4983077	212.16	6.84	3.47	0.10
0.08	3.9687	9.6281	-12393.4296848	210.29	6.78	3.42	0.15
0.10	4.0139	9.6572	-12393.3545583	208.25	6.72	3.38	0.19

The Electronic Properties of Anatase TiO_2 based on B2PLYP

The total and partial density of states (TDOS and PDOS) and electronic structure of anatase TiO_2 for pure and distorted (-0.06 Å) structure is extracted based on B2PLYP/3-21G calculation on large cluster size of $Ti_{159}O_{100}$. As shown in Figure 4, the electronic band structure of the top of the valence band (VB) or HOMO has major contribution from O-p orbital while Ti-d orbital contributes more to the lower levels of the conduction band (CB) or LUMO, which is in good agreement with previous work [18]. This again indicated that B2PLYP calculation is suitable to reflect the electronic properties of anatase TiO_2 .

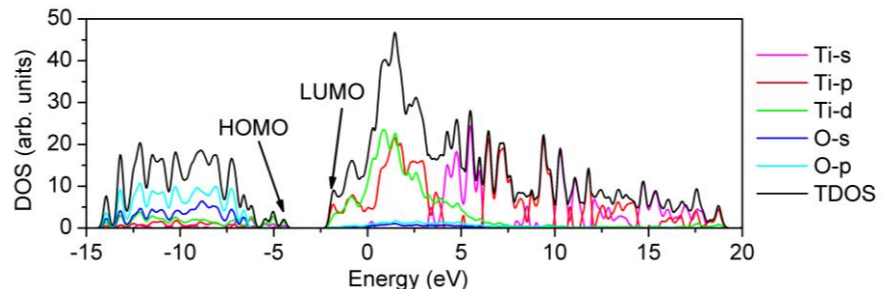


Figure 4. Partial density of states (PDOS) for $Ti_{159}O_{100}$ clusters

Mulliken Charge Transfer Analysis of Anatase TiO₂

Mulliken charge transfer analysis is used in explaining the charge transfer in molecules, molecular polarity and chemical bond strength which are important in the theoretical application [51], such as investigating the charge transfer in TiO₂ after doping [52]. Table 6 shows the Mulliken charge transfer of anatase Ti₁₃O₁₈ cluster using different theoretical methods and basis set. The charge distribution of the atoms involved the charge transfer between the Ti and O atoms in a molecule that act as donor and acceptor atoms, respectively. From the Mulliken charge transfer data analysis, all the Ti atoms exhibit positive charges and all oxygen atoms exhibit negative charges for all DFT and HF methods. The partial negative charge of O atom shows that the O atom attract electron density away from the Ti atom leaving them positively charged. The values obtained with hybrid functionals (B3LYP, B3PW91, PBE1PBE or PBEh1PBE) are lower compared to those obtained with HF (more ionic structure in HF) and, as expected, double-hybrid B2PLYP functionals produced intermediate results, which shows a better representative for charge transfer analysis.

Table 6. Mulliken charge transfer analysis of anatase Ti₁₃O₁₈ cluster using different theoretical methods and basis set

Atom	6-311G(d)					
	B3LYP	B3PW91	PBE1PBE	PBEh1PBE	B2PLYP	HF
Ti	1.11	1.11	1.14	1.13	1.29	1.54
O	-0.82	-0.81	-0.82	-0.82	-0.93	-1.11

Conclusions

Despite the success of DFT exchange-correlation functionals in a wide range of applications, it still suffers many problems including band gap energy estimation of a semiconductor. In the current study, Hartree-Fock, density functional theory and 2nd order Møller-Plesset Perturbation Theory have been employed to investigate the structural and electronic properties of anatase TiO₂ cluster using Gaussian 09 software package. We conclude that B2PLYP double hybrid functional provide better accuracy in predicting the band gap energy of anatase TiO₂ cluster. If one is mainly interested in accurate results of band gap energy, then small anatase cluster Ti₂₁O₃₀ is a good choice, due to the good agreement of band gap energy with experimental results. On the other hand, large anatase supercell Ti₅₉O₁₀₀ will suffer high delocalization error in predicting band gap energy, but this large supercell may be favorable to study the effect of dopants on the band gap energy of anatase TiO₂. Thus, we recommend double-hybrid B2PLYP as a practical choice for predicting the structural and electronic properties for all anatase TiO₂ cluster sizes due to the significant improvement on the band gap and cohesive energy predictions as well as charge transfer analysis when compared to HF and hybrid functionals.

Conflicts of Interest

The authors declare that there is no conflict of interest regarding the publication of this paper.

Acknowledgment

This work was funded by the Internal Funds of Universitas Negeri Malang (UM) for Collaborative Research between Universitas Negeri Malang (UM) and Universiti Teknologi Malaysia (UTM). Furthermore, the authors gratefully acknowledge the Universiti Teknologi MARA under the Research Grant MyRA (600-RMC/GPM LPHD 5/3 (057/2021).

References

- [1] Pandi, K., Preeyanghaa, M., Vinesh, V., Madhavan, J. and Neppolian, B. (2022). Complete photocatalytic degradation of tetracycline by carbon doped TiO₂ supported with stable metal nitrate hydroxide. *Environmental Research*. 207.
- [2] Spătaru, T., Alexandru Mihai, M., Preda, L., Marcu, M., Marian, Radu, M., Dan Becherescu, N., Velea, A., Yassine Zaki, M., Udrea, R., Satulu, V. and Spătaru, N. (2022). Enhanced photoelectrochemical activity of WO₃-decorated native titania films by mild laser treatment. *Applied Surface Science*. 596.
- [3] Tuntithavornwat, S., Saisawang, C., Ratvijitvech, T., Watthanaphanit, A., Hunsom, M. and Kannan, A. M.

- (2024). Recent development of black TiO₂ nanoparticles for photocatalytic H₂ production: An extensive review. *International Journal of Hydrogen Energy*. 55,1559-93.
- [4] Bellotti, V., Daldossi, C., Perilli, D., D'Arienzo, M., Stredansky, M., Di Valentin, C. and Simonutti, R. (2023). Mechanism of sustainable photocatalysis based on doped-titanium dioxide nanoparticles for UV to visible light induced PET-RAFT photo-polymerization. *Journal of Catalysis*. 428.
- [5] Ibrahim, N. S., Leaw, W. L., Mohamad, D., Alias, S. H. and Nur H. (2020). A critical review of metal-doped TiO₂ and its structure–physical properties–photocatalytic activity relationship in hydrogen production. *International Journal of Hydrogen Energy*. 45(53), 28553-65.
- [6] Sheikh Mohd Ghazali, S. A. I., Fatimah, I., Zamil, Z. N., Zulkifli, N. N. and Adam, N. (2023). Graphene quantum dots: A comprehensive overview. Vol. 21, *Open Chemistry*. De Gruyter Open Ltd.
- [7] Alias, S. H., Mohamed, N., Loon, W. and Chandren, S. (2019). Synthesis of carbon self-doped titanium dioxide and its activity in the photocatalytic oxidation of styrene under visible light irradiation. *Malaysian Journal of Fundamental and Applied Sciences*, 15.
- [8] Zhang, L. Y., Yang, J. J. and Han, Y. L. (2022). Novel adsorption-photocatalysis integrated bismuth tungstate modified layered mesoporous titanium dioxide (Bi₂WO₆/LM-TiO₂) composites. *Optical Materials*. 130.
- [9] Palanivelu, K., Im, J. S. and Young-Seaky, L. (2007). Carbon doping of TiO₂ for visible light photo catalysis-A review. *Carbon Science*, 8(3), 214-24.
- [10] Sano, T., Mera, N., Kanai, Y., Nishimoto, C., Tsutsui, S., Hirakawa, T. and Negishi, N. (2012). Origin of visible-light activity of N-doped TiO₂ photocatalyst: Behaviors of N and S atoms in a wet N-doping process. *Applied Catalysis B: Environmental*. 128, 77-83.
- [11] Xiao, H., Tahir-kheli, J. and Goddard, W. A. (2011). Accurate band gaps for semiconductors from density functional theory. *The Journal of Physical Chemistry Letters*, 2, 212-7.
- [12] Ko, K. C., Lamiel-garcía, O., Lee, J. Y. and Illas, F. (2016). Performance of a modified hybrid functional in the simultaneous description of stoichiometric and reduced TiO₂ polymorphs. *Physical Chemistry Chemical Physics: PCCP*, 18(17), 2357-67.
- [13] Gao, H., Ding, C. and Dai, D. (2010). Density functional characterization of C-doped anatase TiO₂ with different oxidation state. *Journal of Molecular Structure: THEOCHEM*, 944(1-3), 156-62.
- [14] Khan, M., Cao, W., Chen, N., Usman, Z., Khan, D. F., Toufiq, A. M. and Khaskheli, M. A. (2013). Influence of tungsten doping concentration on the electronic and optical properties of anatase TiO₂. *Current Applied Physics*, 13(7), 1376-82.
- [15] Lin, Y., Zhu, S., Jiang, Z., Hu, X., Zhang, X., Zhu, H., Fan, J., Mei, T. and Zhang, G. (2013). Electronic and optical properties of S/I-codoped anatase TiO₂ from ab initio calculations. *Solid State Communications*. 171, 17-21.
- [16] Li, M., Zhang, J. and Zhang, Y. (2012). Electronic structure and photocatalytic activity of N/Mo doped anatase TiO₂. *Catalysis Communications*, 29, 175-9.
- [17] Peng L. P., Xu, L. and Xia, Z. C. (2014). Study the high photocatalytic activity of vanadium and phosphorus co-doped TiO₂ from experiment and DFT calculations. *Computational Materials Science*. 83, 309-17.
- [18] Pan, G., Xuejun, Z., Wenfang, Z., Jing, W. and Qingju, L. (2010). First-principle study on anatase TiO₂ codoped with nitrogen and ytterbium. *Journal of Semiconductors*. 31(3), 032001.
- [19] Tsuneda, T. and Hirao, K. (2014). Self-interaction corrections in density functional theory. *Journal of Chemical Physics*, 140(18).
- [20] Bao, J. L., Gagliardi, L. and Truhlar, D. G. (2018). Self-interaction error in density functional theory: An appraisal. *Journal of Physical Chemistry Letters*. 9(9), 2353-8.
- [21] Mori-Sánchez, P., Cohen, A. J. and Yang, W. (2008). Localization and delocalization errors in density functional theory and implications for band-gap prediction. *Physical Review Letters*, 100(146401), 1-4.
- [22] Di Valentin, C. and Pacchioni, G. (2013). Trends in non-metal doping of anatase TiO₂: B, C, N and F. *Catalysis Today*. 206, 12-8.
- [23] Labat, F., Baranek, P., Domain, C., Minot, C. and Adamo, C. (2007). Density functional theory analysis of the structural and electronic properties of TiO₂ rutile and anatase polytypes: Performances of different exchange-correlation functionals. *The Journal of Chemical Physics*. 126(15), 154703.
- [24] Grimme, S. and Neese, F. (2007). Double-hybrid density functional theory for excited electronic states of molecules. *Journal of Chemical Physics*, 127(154116), 1-18.
- [25] Frisch, M. J., Trucks, G. W., Schlegel, H. B., Scuseria, G. E., Robb, M. A., Cheeseman, J. R. *et al.* (2010). Gaussian 09, Revision C.01.
- [26] Atanelov, J., Gruber, C. and Mohn, P. (2015). The electronic and magnetic structure of p-element (C,N) doped rutile-TiO₂; a hybrid DFT study. *Computational Materials Science*, 98, 42-50.
- [27] Gijs Schaftenaar. (2018). Molden.
- [28] Roothan, C. C. J. (1951). New developments in molecular orbital theory. *Reviews of Modern Physics*, 23(2), 69-89.
- [29] Becke, A. D. (1993). Density-functional thermochemistry III. The role of exact exchange. *Journal of Chemical Physics*, 98(7), 5648-52.
- [30] Lee, C., Yang, W. and Parr, R. G. (1988). Development of the Colle-Salvetti correlation-energy formula into a functional of the electron density. *Physical Review B*, 37(2), 785-9.
- [31] Miehlich, B., Savin, A., Stoll, H. and Preuss, H. (1989). Results obtained with the correlation energy density functionals of Becke and Lee, Yang and Parr. *Chemical Physics Letters*, 157(3), 200-6.
- [32] Perdew, J. P., Jackson, K. A., Pederson, M. R., Singh, D. J. and Fiolhais, C. (1992). Atoms, molecules, solids, and surfaces: Applications of the GGA for exchange and correlation. *Physical Review B*, 46(11), 6671.
- [33] Shi, J. M., Peeters, F. M., Hai, G. Q. and Devreese, J. T. (1991). Donor transition energy in GaAs superlattices in a magnetic field along the growth axis. *Physical Review B*, 44(11), 5692-702.
- [34] Perdew, J., Burke, K. and Wang, Y. (1996). Generalized gradient approximation for the exchange-correlation hole of a many-electron system. *Physical Review B*, 54(23), 16533-9.
- [35] Perdew, J. P., Burke, K. and Ernzerhof, M. (1996). Generalized gradient approximation made simple. *Physical*

- Review Letters*, 77(18), 3865-8.
- [36] Perdew, J. P., Burke, K. and Ernzerhof, M. (1997). Errata: Generalized gradient approximation made simple. *Physical Review Letters*, 78(7), 1396.
- [37] Adamo, C. and Barone, V. (1999). Toward reliable density functional methods without adjustable parameters: The PBE0 model. *Journal of Chemical Physics*, 110(13), 6158-70.
- [38] Ernzerhof, M. and Perdew, J. P. (1998). Generalized gradient approximation to the angle- and system-averaged exchange hole. *Journal of Chemical Physics*, 109(9), 3313-20.
- [39] Schwabe, T. and Grimme, S. (2007). Double-hybrid density functionals with long-range dispersion corrections: higher accuracy and extended applicability. *Physical Chemistry Chemical Physics: PCCP*, 9(26), 3397-406.
- [40] Frisch, M. J., Head-Gordon, M. and People, J. A. (1990). Semi-direct algorithms for the MP2 energy and gradient. *Chemical Physics Letters*, 166(3), 281-9.
- [41] Head-Gordon, M., People, J. A. and Frisch, M. J. (1988). MP2 energy evaluation by direct methods. *Chemical Physics Letters*, 153(6), 503-6.
- [42] Sæbø, S. and Almlöf, J. (1989). Avoiding the integral storage bottleneck in LCAO calculations of electron correlation. *Chemical Physics Letters*, 154(1), 83-9.
- [43] Head-Gordon, M. and Head-Gordon, T. (1994). Analytic MP2 frequencies without fifth-order storage. Theory and application to bifurcated hydrogen bonds in the water hexamer. *Chemical Physics Letters*, 220(1-2), 122-8.
- [44] Parra, R. D. and Farrell, H. H. (2009). Binding energy of metal oxide nanoparticles. *The Journal of Physical Chemistry C*, 113(12), 4786-91.
- [45] Zhu, H. X. and Liu, J.-M. (2014). Electronic and optical properties of C and Nb co-doped anatase TiO₂. *Computational Materials Science*, 85, 164-71.
- [46] Xi, X., Dong, P., Pei, H., Hou, G., Zhang, Q., Guan, R., Xu, N. and Wang, Y. (2014). Density functional study of X monodoped and codoped (X = C, N, S, F) anatase TiO₂. *Computational Materials Science*, 93, 1-5.
- [47] Zheng, X., Cohen, A. J., Mori-Sánchez, P., Hu, X. and Yang, W. (2011). Improving band gap prediction in density functional theory from molecules to solids. *Physical Review Letters*, 107(2), 1-4.
- [48] Hua Gui, Y., Cheng Hua, S., Shi Zhang, Q., Jin, Z., Gang, L., Sean Campbell, S., Hui Ming, C. and Gao Qing, L. (2008). Supplementary Information, Anatase TiO₂ single crystals with a large percentage of reactive facets. *Nature*, 453(7195), 638-41.
- [49] Erdin, S., Lin, Y., Halley, J. W., Zapol, P., Redfern, P. and Curtiss, L. (2007). Self-consistent tight binding molecular dynamics study of TiO₂ nanoclusters in water. *Journal of Electroanalytical Chemistry*, 607(1-2), 147-57.
- [50] Lazzeri, M., Vittadini, A. and Selloni, A. (2001). Structure and energetics of stoichiometric TiO₂ anatase surfaces. *Physical Review B*, 63(155409), 1-9.
- [51] Xu, B., Guo, X. and Tian, Y. (2009). Universal quantification of chemical bond strength and its application to low dimensional materials. In: *WwwIntechopenCom*.
- [52] Kumar, N., Hazarika, S. N., Limbu, S., Boruah, R., Deb, P., Namsa, N. D. and Das, S. K. (2015). Hydrothermal synthesis of anatase titanium dioxide mesoporous microspheres and their antimicrobial activity. *Microporous and Mesoporous Materials*, 213, 181-7.